X. Optimal Transport-based Method

Young-geun Kim

Department of Statistics and Probability

STT 997 (SS 2025)

MICHIGAN STATE UNIVERSITY

Introduction

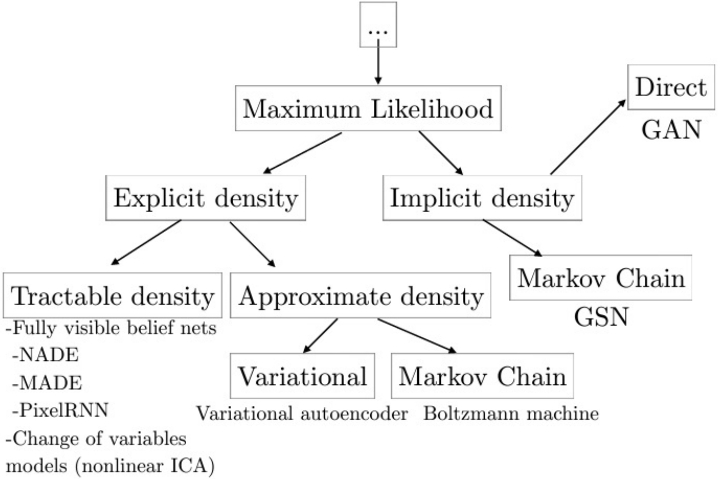

The figure is from Goodfellow (2016).

Introduction

***f* divergence -based methods** → Integral Probability Metric -based methods → Wasserstein Distance -based methods → Fisher Divergence -based methods

(*a*) Blurry generation results from VAEs

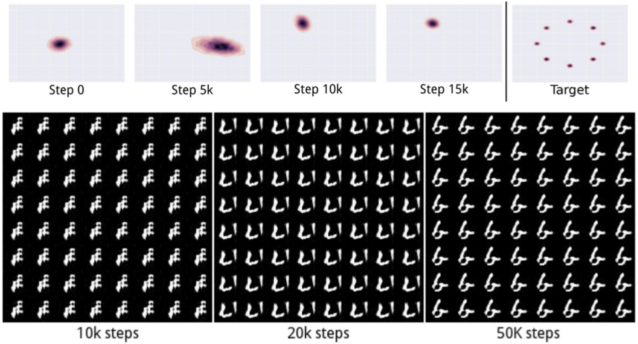

(*b*) Mode collapse results from GANs

Images are edited from Tolstikhin et al. (2018) and Metz et al. (2017).

Introduction

f divergence -based methods | **Integral Probability Metric -based methods** | **Wasserstein Distance -based methods** | **Fisher Divergence -based methods**

- The mode collapse phenomenon in GANs demonstrates that the p_θ fails in capturing the support of p_n.
- Several works have criticized f-divergence,

$$\mathcal{D}_f(p_n \| p_\theta) = \int f\left(\frac{p_n(\vec{x})}{p_\theta(\vec{x})}\right) p_\theta(\vec{x})\, d\vec{x},$$

  pointing out that it is based on the density ratio p_n / p_θ, and this dependency may be a reason for the observed failures in f-divergence-based methods.

Introduction

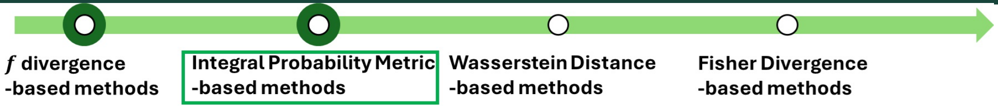

- As an alternative to density ratios, a line of work has proposed focusing on discrepancy measures that are effective regardless of the differences between the supports of p_n and p_θ.
- For example, Generative Moment Matching Networks (Li et al., 2015) aim to minimize:

$$\left\| \int \varphi(\vec{x}) d\mathbb{P}_n(\vec{x}) - \int \varphi(\vec{x}) d\mathbb{P}_\theta(\vec{x}) \right\|^2 \tag{1}$$

  where the integrated terms $\varphi(\vec{x})$ represent vectors of finite moments, e.g., $\varphi(x) = (c, \sqrt{2}cx, x^2)^T$ in the univariate case with second-order moments.
- This loss function is a special case of integral probability metrics, $\gamma_{\mathcal{F}}(p_n, p_\theta)$, where $\mathcal{F}$ denotes a set of summary statistics functions, such as moments.

Integral Probability Metric

- The IPMs can be expressed as:

$$\gamma_{\mathcal{F}}(\mathbb{P}, \mathbb{Q}) := \sup_{f \in \mathcal{F}} \left| \int f(\vec{x})\, d\mathbb{P}(\vec{x}) - \int f(\vec{x})\, d\mathbb{Q}(\vec{x}) \right|$$

where $\mathcal{F}$ is a class of real-valued functions, and $\mathbb{P}$ and $\mathbb{Q}$ are probability measures.

Integral Probability Metric

- **Total Variation Distance**: The total variation distance, $\delta(p, q) = \frac{1}{2} \int \left| p(\vec{x}) - q(\vec{x}) \right| d\vec{x}$, has an alternative expression:

$$\sup_{A \in \mathcal{A}} \left| \mathbb{P}(A) - \mathbb{Q}(A) \right| = \sup_{A \in \mathcal{A}} \left| \int I(\vec{x} \in A) d\mathbb{P}(\vec{x}) - \int I(\vec{x} \in A) d\mathbb{Q}(\vec{x}) \right|$$

  where $\mathcal{A}$ is the corresponding σ-algebra. Thus, the total variation is the IPM using the set of indicator functions for all events.

- **Earth Mover's Distance**: When $\mathcal{F}$ consists of all 1-Lipschitz continuous functions, $\gamma_{\mathcal{F}}(\mathbb{P}, \mathbb{Q})$ corresponds to the Earth mover's distance (or 1-Wasserstein distance), a special case of Wasserstein distances. Further details will be discussed in the subsequent subsection on Wasserstein distances.

Integral Probability Metric

- **Maximum Mean Discrepancy (MMD)**: We denote the kernel mean by $\mu_{\mathbb{P}}(\vec{x}) := \int k(\vec{x}', \vec{x}) d\mathbb{P}(\vec{x}')$. Then, the MMD is defined as the difference between kernel means in $\mathcal{H}$, the RKHS specified by k:

$$\mathrm{MMD}_k(\mathbb{P}, \mathbb{Q}) := \|\mu_{\mathbb{P}} - \mu_{\mathbb{Q}}\|_{\mathcal{H}}.$$

  MMD builds a kernel-based test statistic for a two-sample test:

$$H_0 : \mathbb{P} = \mathbb{Q} \text{ vs. } H_1 : \mathbb{P} \neq \mathbb{Q}.$$

- The MMD has important alternative representations:
  1. **IPM:** $\mathrm{MMD}_k(\mathbb{P}, \mathbb{Q}) = \sup_{\|f\|_{\mathcal{H}} \leq 1} \left(\int f(\vec{x}) d\mathbb{P}(\vec{x}) - \int f(\vec{x}) d\mathbb{Q}(\vec{x}) \right)$.
  2. **Kernel function form:**

$$\begin{aligned} &\mathrm{MMD}_k^2(\mathbb{P}, \mathbb{Q}) \\ &= \int k(\vec{x}, \vec{x}') d\mathbb{P}(\vec{x}) d\mathbb{P}(\vec{x}') - 2 \int k(\vec{x}, \vec{y}) d\mathbb{P}(\vec{x}) d\mathbb{Q}(\vec{y}) + \int k(\vec{y}, \vec{y}') d\mathbb{Q}(\vec{y}) d\mathbb{Q}(\vec{y}'). \end{aligned} \tag{2}$$

MMD: Generative Moment Matching Network

1. **Generative Moment Matching Network (GMMN)**: GMMNs (Li et al., 2015) propose to use empirical estimators as loss functions to train generative models rather than introducing adversarial networks as in GANs.

- Given $(\vec{x}_i)_{i=1}^{B}$ and $(G_\theta(\vec{z}_i))_{i=1}^{B}$, minibatch samples of size B from $\mathbb{P}_n$ and $\mathbb{P}_\theta$ respectively, the minibatch-based empirical estimators for $\mathrm{MMD}_k^2(\mathbb{P}_n, \mathbb{P}_\theta)$ can be expressed as

$$\begin{aligned} &\frac{1}{B(B-1)} \sum_{i=1}^{B} \sum_{j \neq i}^{B} k(\vec{x}_i, \vec{x}_j) - \frac{2}{B^2} \sum_{i=1}^{B} \sum_{j=1}^{B} k(\vec{x}_i, G_\theta(\vec{z}_j)) \\ &+ \frac{1}{B(B-1)} \sum_{i=1}^{B} \sum_{j \neq i}^{B} k(G_\theta(\vec{z}_i), G_\theta(\vec{z}_j)). \end{aligned} \tag{3}$$

- GMMNs used a mixture of multiple Gaussian kernels with various bandwidth parameters.

MMD: Generative Moment Matching Network

- Minimizing $\mathrm{MMD}_k(\mathbb{P}_n, \mathbb{P}_\theta)$ can be interpreted as matching moments between $\mathbb{P}_n$ and $\mathbb{P}_\theta$.
- Let k be the kernel that defines the MMD, and let $\varphi(\vec{x})$[1] represent the corresponding kernel feature mapping, i.e.,

$$k(\vec{x}, \vec{x}') = \varphi(\vec{x})^\top \varphi(\vec{x}') \tag{4}$$

- For a univariate example, consider $k(x, x') = (xx' + c)^2$ for some $c > 0$. The feature mapping $\varphi(x) = (c, \sqrt{2c}x, x^2)^\top$ satisfies Equation (4). Kernels with higher degrees allow for covering higher-order moments.
- The loss of GMMNs, minibatch-based empirical estimators for (squared) MMD, can be expressed as

$$\|B^{-1} \sum_{i=1}^{B} \varphi(\vec{x}_i) - B^{-1} \sum_{i=1}^{B} \varphi(G_\theta(\vec{z}_i))\|^2. \tag{5}$$

[1]The symbol ϕ is more commonly used, but we use φ here to avoid confusion with parameters for auxiliary networks, e.g., the discriminator in GANs.

MMD: MMD GAN

2. **MMD GAN**:

- GMMNs face challenges in selecting effective kernels. MMD GANs (Li et al., 2017) overcome this limitation by introducing adversarial kernel learning.
- MMD GANs aim to target $\max_{k \in \mathcal{K}} \text{MMD}_k(\mathbb{P}_n, \mathbb{P}_\theta)$, where $\mathcal{K}$ is a class of kernel functions.
- To model an expressive class $\mathcal{K}$, MMD GANs employ a neural network E_ϕ to define $(k \circ E_\phi)(\vec{x}, \vec{x}') := k(E_\phi(\vec{x}), E_\phi(\vec{x}'))$, targeting:

$$\max_{\phi} \text{MMD}_{k \circ E_\phi}(\mathbb{P}_n, \mathbb{P}_\theta). \tag{6}$$

- The injectivity of E_ϕ is crucial to retain the important properties of MMDs with usual kernels. MMD-GANs incorporate an encoder architecture for E_ϕ, add a decoder, and introduce a reconstruction error-based penalty term to enforce the injectivity.

Other IPMs

3. **Methods using Other IPMs**:

- One of the main challenges in using IPMs,

$$\gamma_{\mathcal{F}}(\mathbb{P}_n, \mathbb{P}_\theta) := \sup_{f \in \mathcal{F}} \left| \int f(\vec{x})\, d\mathbb{P}_n(\vec{x}) - \int f(\vec{x})\, d\mathbb{P}_\theta(\vec{x}) \right|,$$

  lies in approximating the supremum over the function class $\mathcal{F}$.
- While MMD has a tractable representation that allows for the direct use of its empirical estimators, this is not the case for more general IPMs.
- Most methods targeting other IPMs employ neural networks to model elements within $\mathcal{F}$. Notably, Wasserstein GANs (Arjovsky et al., 2017) have become one of the most popular methods targeting the 1-Wasserstein distance.

Outline

Optimal Transport

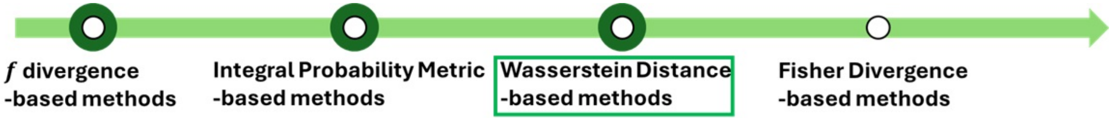

- Another line of work has targeted Wasserstein distances from an optimal transport perspective.
- Useful materials include:
  1. *Optimal transport: old and new* (Villani et al., 2009)
  2. *Optimal transport for applied mathematicians* (Santambrogio, 2015)

Images are edited from Santambrogio (2015).

Motivating Example: Monge Problem

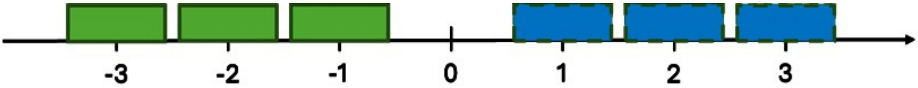

- *Optimal Transport* is a mathematical problem focused on identifying maps that most efficiently move one distribution of mass to another and investigating their properties.
- Let's consider a toy example of moving green bold boxes on the left to blue dashed-box regions on the right.
- Which way is more efficient?
  1. T_1: $T_1(-3) = 1$, $T_1(-2) = 2$, and $T_1(-1) = 3$
  2. T_2: $T_2(-3) = 3$, $T_2(-2) = 2$, and $T_2(-1) = 1$

Motivating Example: Monge Problem

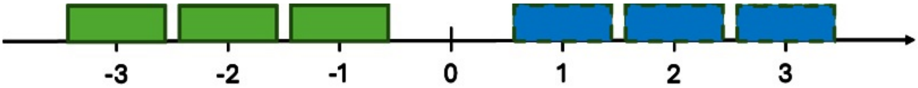

- The answer depends on criteria. When we consider the squared L_2-distance between the original green boxes and their transportation results:

$$\begin{aligned}&\left((-3-T_1(-3))^2+(-2-T_1(-2))^2+(-1-T_1(-1))^2\right)/3\\&=\left((-3-1)^2+(-2-2)^2+(-1-3)^2\right)/3=16\end{aligned}\tag{7}$$

$$\begin{aligned}&\left((-3-T_2(-3))^2+(-2-T_2(-2))^2+(-1-T_2(-1))^2\right)/3\\&=\left((-3-3)^2+(-2-2)^2+(-1-1)^2\right)/3=56/3\end{aligned}\tag{8}$$

Q: How many (transportation) maps are there?
Q: What happens when we consider the L_1-distance?

Motivating Example: Monge Problem

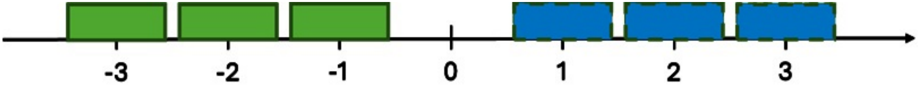

- The *Monge Problem* is a classical formulation in Optimal Transport: Given two probability measures $\mathbb{P}$ and $\mathbb{Q}$, and a cost function $c(\cdot,\cdot) : \mathcal{X} \times \mathcal{X} \to \mathbb{R}$, the optimal transportation cost is defined as:

$$\min_{T:\mathbb{P}(T(\vec{x}))=\mathbb{Q}(\vec{x})} \int c(\vec{x}, T(\vec{x}))d\mathbb{P}(\vec{x}) \tag{9}$$

  The constraint $\mathbb{P}(T(\vec{x})) = \mathbb{Q}(\vec{x})$ represents the push-forward operation $T\#\mathbb{P} = \mathbb{Q}$. Here, the optimal solutions are referred to as *optimal transport maps*.
- When the cost function is the squared L_2-distance, $c(\vec{x}, \vec{x}') = \|\vec{x} - \vec{x}'\|^2$, T_1 is the unique optimal transport map. In the univariate case, the transport map that moves percentiles to corresponding percentiles is optimal.

Motivating Example: Optimal Transportation Costs as Measures of Generation Quality

			
	1/3	0	0
	0	1/3	0
	0	0	1/3

Joint Distribution

			
	0.10	0.30	0.40
	0.40	0.05	0.25
	0.25	0.30	0.10

Transportation Cost

$$
\begin{aligned}
&\big(0.10 \times (1/3) + 0.30 \times 0 + 0.40 \times 0\big) \\
&+ \big(0.40 \times 0 + 0.05 \times (1/3) + 0.25 \times 0\big) \\
&+ \big(0.25 \times 0 + 0.30 \times 0 + 0.10 \times (1/3)\big) = 0.08
\end{aligned}
$$

Motivating Example: Kantorovich Problem

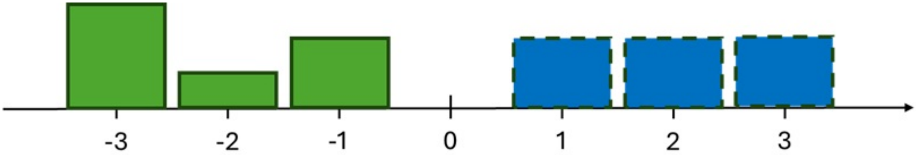

- The constraint on the optimal transport map, $\mathbb{P}(T(\vec{x})) = \mathbb{Q}(\vec{x})$, generally poses challenges in defining the optimal transportation cost.
- The *Kantorovich Problem* is a generalization of the Monge Problem to alleviate these challenges.

Motivating Example: Kantorovich Problem

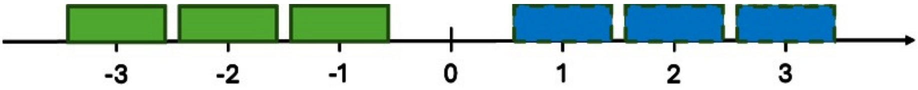

- In the first example, the joint distribution of $(x, T_1(x))$ can be expressed as:

(Source, Target)	1	2	3	Total
-3	1/3	0	0	1/3
-2	0	1/3	0	1/3
-1	0	0	1/3	1/3
Total	1/3	1/3	1/3	1

- That is, each (deterministic) transport map identifies the corresponding joint distribution of the source data and their transported results.

Motivating Example: Kantorovich Problem

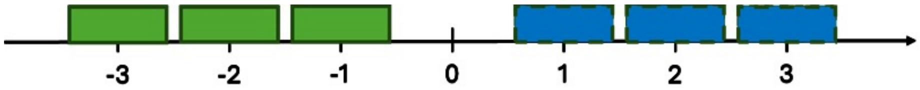

- We denote the joint probability measure by $\pi(\cdot,\cdot)$ s.t. $\pi(\cdot,\Omega_{\vec{X}'}) = \mathbb{P}(\cdot)$ and $\pi(\Omega_{\vec{X}'},\cdot) = \mathbb{Q}(\cdot)$. Then, the transportation cost can be expressed as $\int c(\vec{x},\vec{x}')d\pi(\vec{x},\vec{x}')$.
- The Kantorovich Problem involves minimizing transportation costs among all joint distributions whose marginals are the source and target data distributions:

(Source, Target)	1	2	3	Total
-3	$p_{(-3,1)}$	$p_{(-3,2)}$	$p_{(-3,3)}$	$1/3$
-2	$p_{(-2,1)}$	$p_{(-2,2)}$	$p_{(-2,3)}$	$1/3$
-1	$p_{(-1,1)}$	$p_{(-1,2)}$	$p_{(-1,3)}$	$1/3$
Total	$1/3$	$1/3$	$1/3$	1

Motivating Example: Kantorovich Problem

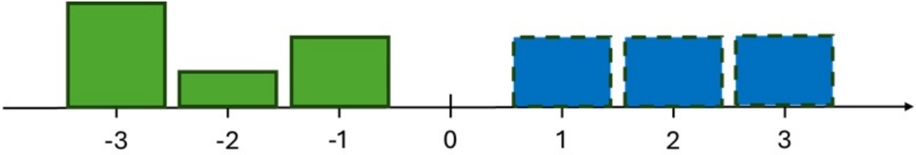

(Source, Target)	1	2	3	Total
-3	$p_{(-3,1)}$	$p_{(-3,2)}$	$p_{(-3,3)}$	$1/2$
-2	$p_{(-2,1)}$	$p_{(-2,2)}$	$p_{(-2,3)}$	$1/6$
-1	$p_{(-1,1)}$	$p_{(-1,2)}$	$p_{(-1,3)}$	$1/3$
Total	$1/3$	$1/3$	$1/3$	1

Motivating Example: Kantorovich Problem

$$
\begin{aligned}
&\min_{p_{(-3,1)},\cdots,p_{(-1,3)}} \left(c(-3,1)p_{(-3,1)} + \cdots + c(-1,3)p_{(-1,3)} \right) \\
&\text{subject to} \\
&\quad p_{(-3,1)} + p_{(-3,2)} + p_{(-3,3)} = 1/2, \\
&\quad p_{(-2,1)} + p_{(-2,2)} + p_{(-2,3)} = 1/6, \\
&\quad p_{(-1,1)} + p_{(-1,2)} + p_{(-1,3)} = 1/3, \\
&\quad p_{(-3,1)} + p_{(-2,1)} + p_{(-1,1)} = 1/3, \\
&\quad p_{(-3,2)} + p_{(-2,2)} + p_{(-1,2)} = 1/3, \\
&\quad p_{(-3,3)} + p_{(-2,3)} + p_{(-1,3)} = 1/3, \\
&\quad p_{(-3,1)} \geq 0, \ldots, p_{(-1,3)} \geq 0.
\end{aligned} \tag{10}
$$

Wasserstein Distance

- The p-**Wasserstein distance** is defined as:

$$W_p(\mathbb{P}, \mathbb{Q}; d) := \left(\inf_{\pi \in \Pi(\mathbb{P}, \mathbb{Q})} \int d^p(\vec{x}, \vec{x}')\, d\pi(\vec{x}, \vec{x}') \right)^{1/p}$$

where $p \in [1, \infty)$, d is a metric defined on $\mathcal{X}$,[2] and $\Pi(\mathbb{P}, \mathbb{Q})$ is the set of all joint probability measures whose marginals are $\mathbb{P}$ and $\mathbb{Q}$.

- Under some conditions, there exists an optimal transport map T^* that satisfies:
  1. $W_p(\mathbb{P}, \mathbb{Q}; d) = \left(\int d^p(\vec{x}, T^*(\vec{x}))d\mathbb{P}(\vec{x})\right)^{1/p}$
  2. $\mathbb{P}(T^*(\vec{x})) = \mathbb{Q}(\vec{x})$

  That is, Monge Problem can be equivalent to the Kantorovich Problem, and together they are simply referred to as the Monge-Kantorovich Problem.

[2] The Kantorovich Problem is generally defined with the cost function c.

Wasserstein Distance

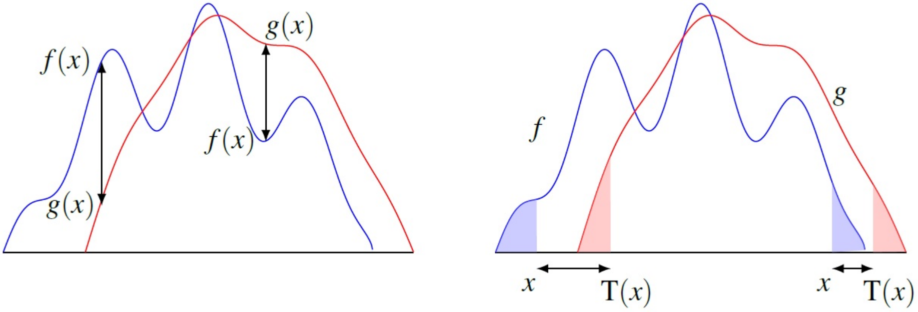

- The f-divergence utilizes density-ratios to quantify discrepancies between distributions.
- In contrast, Wasserstein distances utilize transportation costs.

The figure is from Santambrogio (2015).

Wasserstein Distance

- For example, when d is the Euclidean norm, W_p becomes the Mallows metric (Mallows, 1972), and has played an important role in deriving asymptotic properties of bootstrap estimators (Bickel and Freedman, 1981; Freedman, 1981).
- Wasserstein distances effectively quantify differences between high-dimensional distributions when their supports are in low-dimensional manifolds.

Example

(Example 1 in Arjovsky et al., 2017) Let $Z \sim U[0,1]$, $\vec{X} = (0, Z)^T$, and $G_\theta(Z) = (\theta, Z)^T$.

- Intuitively, $\mathcal{D}(\mathbb{P}_{n=\infty}, \mathbb{P}_\theta)$ should decrease as θ vanishes.
    - $W_p(\mathbb{P}_{n=\infty}, \mathbb{P}_\theta; |\cdot|) = |\theta|$
    - $\mathrm{JS}(\mathbb{P}_{n=\infty} \parallel \mathbb{P}_\theta) = \log 2$ if $\theta \neq 0$ and 0 if $\theta = 0$
    - $\mathrm{KL}(\mathbb{P}_{n=\infty} \parallel \mathbb{P}_\theta) = \infty$ if $\theta \neq 0$ and 0 if $\theta = 0$
    - $\delta(\mathbb{P}_{n=\infty}, \mathbb{P}_\theta) = 1$ if $\theta \neq 0$ and 0 if $\theta = 0$

1−Wasserstein Distance: Duality

- When $p = 1$ (called *Earth Mover's Distance*), duality holds (Villani et al., 2009; Villani, 2021):

$$W_1(\mathbb{P}, \mathbb{Q}; d) = \sup_{f,g: f(\vec{x}) + g(\vec{x}') \leq d(\vec{x}, \vec{x}')} \left(\int f(\vec{x}) d\mathbb{P}(\vec{x}) + \int g(\vec{x}') d\mathbb{Q}(\vec{x}') \right). \quad (11)$$

- When we further assume that $d(\vec{x}, \vec{x}') = \|\vec{x} - \vec{x}'\|$ for some norm $\|\cdot\|$, the dual form can be re-expressed as:

$$W_1(\mathbb{P}, \mathbb{Q}; d) = \sup_{\mathrm{Lip}(f) \leq 1} \int f(\vec{x}) d\mathbb{P}(\vec{x}) - \int f(\vec{x}) d\mathbb{Q}(\vec{x}) \quad (12)$$

where $\mathrm{Lip}(f) := \max\{C \big| |f(\vec{x}) - f(\vec{x}')| \leq C\|\vec{x} - \vec{x}\|\}$ represents the Lipschitz constant of f. Note that this dual form implies that W_1 is an IPM.

Duality: Sketch of Proof

$\sup_{f,g}\left(\int f(\vec{x})d\mathbb{P}(\vec{x}) + \int g(\vec{x}')d\mathbb{Q}(\vec{x}') - \int \left(f(\vec{x}) + g(\vec{x}')\right)\pi(\vec{x},\vec{x}')\right) = 0$ when $\pi \in \Pi(\mathbb{P},\mathbb{Q})$ and $= \infty$ otherwise, which implies:

$$
\begin{aligned}
&\inf_{\pi\in\Pi(\mathbb{P},\mathbb{Q})} \int d(\vec{x},\vec{x}')d\pi(\vec{x},\vec{x}') \\
&= \inf_{\pi\in\Pi(\mathbb{P},\mathbb{Q})} \Bigg(\int d(\vec{x},\vec{x}')d\pi(\vec{x},\vec{x}') \\
&\qquad + \sup_{f,g} \left(\int f(\vec{x})d\mathbb{P}(\vec{x}) + \int g(\vec{x}')d\mathbb{Q}(\vec{x}') - \int \left(f(\vec{x}) + g(\vec{x}')\right) d\pi(\vec{x},\vec{x}') \right) \Bigg) \\
&= \inf_{\pi\in\Pi(\mathbb{P},\mathbb{Q})} \sup_{f,g} \Bigg(\int d(\vec{x},\vec{x}')d\pi(\vec{x},\vec{x}') + \int f(\vec{x})d\mathbb{P}(\vec{x}) + \int g(\vec{x}')d\mathbb{Q}(\vec{x}') \\
&\qquad - \int \left(f(\vec{x}) + g(\vec{x}')\right) d\pi(\vec{x},\vec{x}') \Bigg).
\end{aligned}
$$

Duality: Sketch of Proof

Now, by exchanging the infimum and supremum:[3]

$$
\begin{aligned}
&\inf_{\pi\in\Pi(\mathbb{P},\mathbb{Q})} \sup_{f,g} \Bigg(\int d(\vec{x},\vec{x}') d\pi(\vec{x},\vec{x}') + \int f(\vec{x}) d\mathbb{P}(\vec{x}) + \int g(\vec{x}') d\mathbb{Q}(\vec{x}') \\
&\qquad - \int \Big(f(\vec{x}) + g(\vec{x}') \Big)\, d\pi(\vec{x},\vec{x}') \Bigg) \\
&= \sup_{f,g} \inf_{\pi\geq 0} \Bigg(\int d(\vec{x},\vec{x}') d\pi(\vec{x},\vec{x}') + \int f(\vec{x}) d\mathbb{P}(\vec{x}) + \int g(\vec{x}') d\mathbb{Q}(\vec{x}') \\
&\qquad - \int \Big(f(\vec{x}) + g(\vec{x}') \Big)\, d\pi(\vec{x},\vec{x}') \Bigg) \\
&= \sup_{f,g} \Bigg(\int f(\vec{x}) d\mathbb{P}(\vec{x}) + \int g(\vec{x}') d\mathbb{Q}(\vec{x}') + \inf_{\pi\geq 0} \int \Big(d(\vec{x},\vec{x}') - f(\vec{x}) - g(\vec{x}') \Big)\, d\pi(\vec{x},\vec{x}') \Bigg).
\end{aligned}
$$

[3] See Section 1.2. in Santambrogio (2015) for details on conditions to exchange them.

Duality: Sketch of Proof

Note that $\inf_{\pi \geq 0} \int \left(d(\vec{x}, \vec{x}') - f(\vec{x}) - g(\vec{x}')\right) d\pi(\vec{x}, \vec{x}') = 0$ if $f(\vec{x}) + g(\vec{x}') \leq d(\vec{x}, \vec{x}')$ for all $(\vec{x}, \vec{x}')$ and $= -\infty$ otherwise. This implies:

$$
\begin{aligned}
&\sup_{f,g} \left(\int f(\vec{x}) d\mathbb{P}(\vec{x}) + \int g(\vec{x}') d\mathbb{Q}(\vec{x}') + \inf_{\pi \geq 0} \int \Big(d(\vec{x}, \vec{x}') - f(\vec{x}) - g(\vec{x}') \Big) \, d\pi(\vec{x}, \vec{x}') \right) \\
&= \sup_{f,g : f(\vec{x}) + g(\vec{x}') \leq d(\vec{x}, \vec{x}')} \left(\int f(\vec{x}) d\mathbb{P}(\vec{x}) + \int g(\vec{x}') d\mathbb{Q}(\vec{x}') \right).
\end{aligned}
$$

Duality: Sketch of Proof

Next, we show that:

$$\begin{aligned} W_1(\mathbb{P}, \mathbb{Q}; d) &= \sup_{f,g: f(\vec{x})+g(\vec{x}')\leq d(\vec{x},\vec{x}')} \left(\int f(\vec{x}) d\mathbb{P}(\vec{x}) + \int g(\vec{x}') d\mathbb{Q}(\vec{x}') \right) \\ &= \sup_{\mathrm{Lip}(f)\leq 1} \int f(\vec{x}) d\mathbb{P}(\vec{x}) - \int f(\vec{x}) d\mathbb{Q}(\vec{x}). \end{aligned} \tag{13}$$

when we further assume that $d(\vec{x}, \vec{x}') = \|\vec{x} - \vec{x}'\|$ for some norm $\|\cdot\|$.
(i) LHS $\leq$ RHS: For any f and g s.t. $f(\vec{x}) + g(\vec{x}') \leq d(\vec{x}, \vec{x}')$ for all $(\vec{x}, \vec{x}')$,

$$f(\vec{x}) \leq f^d(\vec{x}) := \inf_{\vec{x}'} \left(d(\vec{x}, \vec{x}') - g(\vec{x}') \right) \leq d(\vec{x}, \vec{x}) - g(\vec{x}) = -g(\vec{x}). \tag{14}$$

This implies $\int f(\vec{x}) d\mathbb{P}(\vec{x}) + \int g(\vec{x}') d\mathbb{Q}(\vec{x}') \leq \int f^d(\vec{x}) d\mathbb{P}(\vec{x}) - \int f^d(\vec{x}) d\mathbb{Q}(\vec{x})$.

Duality: Sketch of Proof

Here, f^d is 1−Lipschitz continuous because:

$$f^d(\vec{x}_1) \le \inf_{\vec{x}'} \left(d(\vec{x}_1, \vec{x}_2) + d(\vec{x}_2, \vec{x}') - g(\vec{x}') \right) = d(\vec{x}_1, \vec{x}_2) + f^d(\vec{x}_2) \tag{15}$$

and $d(\vec{x}_1, \vec{x}_2) = d(\vec{x}_2, \vec{x}_1)$. This implies $\int f(\vec{x}) d\mathbb{P}(\vec{x}) + \int g(\vec{x}') d\mathbb{Q}(\vec{x}') \le$ RHS, which concludes the proof for LHS $\le$ RHS.

(ii) LHS $\geq$ RHS: For any 1-Lipschitz continuous function f and $\pi \in \Pi(\mathbb{P}, \mathbb{Q})$,

$$\begin{aligned} \int d(\vec{x}, \vec{x}') d\pi(\vec{x}, \vec{x}') &\ge \int \left(f(\vec{x}) - f(\vec{x}') \right) d\pi(\vec{x}, \vec{x}') \\ &= \int f(\vec{x}) d\mathbb{P}(\vec{x}) - \int f(\vec{x}) d\mathbb{Q}(\vec{x}). \end{aligned} \tag{16}$$

Now, sequentially taking the infimum over $\pi \in \Pi(\mathbb{P}, \mathbb{Q})$ and the supremum over $f : \mathrm{Lip}(f) \le 1$ yields LHS $\ge$ RHS.

Primal vs. Dual Problems

- For general cases with cost function c:
  1. (Primal) $\inf_{\pi \in \Pi(\mathbb{P},\mathbb{Q})} \int c(\vec{x}, \vec{x}')d\pi(\vec{x}, \vec{x}')$
  2. (Dual) $\sup_{f,g: f(\vec{x})+g(\vec{x}') \leq c(\vec{x},\vec{x}')} \int f(\vec{x})d\mathbb{P}(\vec{x}) + \int g(\vec{x}')d\mathbb{Q}(\vec{x}')$
- When $d(\vec{x}, \vec{x}') = \|\vec{x} - \vec{x}'\|$:
  1. (Primal) $W_1(\mathbb{P}, \mathbb{Q}; d) = \inf_{\pi \in \Pi(\mathbb{P},\mathbb{Q})} \int d(\vec{x}, \vec{x}')d\pi(\vec{x}, \vec{x}')$
  2. (Dual) $W_1(\mathbb{P}, \mathbb{Q}; d) = \sup_{\mathrm{Lip}(f) \leq 1} \int f(\vec{x})d\mathbb{P}(\vec{x}) - \int f(\vec{x})d\mathbb{Q}(\vec{x})$

Multi-marginal Transport Problem

- The optimal transportation cost is generally defined for multiple distributions as follows:
  1. (Primal)

$$\inf_{\pi \in \Pi(\mathbb{P}^{(1)}, \ldots, \mathbb{P}^{(M)})} \int c(\vec{x}^{(1)}, \ldots, \vec{x}^{(M)}) d\pi(\vec{x}^{(1)}, \ldots, \vec{x}^{(M)}) \tag{17}$$

     where $\Pi(\mathbb{P}^{(1)}, \ldots, \mathbb{P}^{(M)})$ represents the set of all joint probability measures whose marginals are $\mathbb{P}^{(1)}, \ldots, \mathbb{P}^{(M)}$.
  2. (Dual)

$$\sup_{f_1, \ldots, f_M : f_1(\vec{x}^{(1)}) + \cdots + f_M(\vec{x}^{(M)}) \leq c(\vec{x}^{(1)}, \ldots, \vec{x}^{(M)})} \sum_{m=1}^{M} \int f_m(\vec{x}^{(m)}) d\mathbb{P}^{(m)}(\vec{x}^{(m)}) \tag{18}$$

Outline

1-Wasserstein Distance: Wasserstein GAN

1. **Wasserstein GAN (WGAN)**: WGANs model the class of 1-Lipschitz continuous functions using neural networks, denoted by f_ϕ, with the goal of

$$\min_{\theta} \max_{f_\phi} \left(\int f_\phi(\vec{x})\, d\mathbb{P}_n(\vec{x}) - \int f_\phi(\vec{x})\, d\mathbb{P}_\theta(\vec{x}) \right). \tag{19}$$

- When the set $\{f_\phi \mid \phi \in \Phi\}$ perfectly approximates the set $\{f \mid \|f\|_L \leq 1\}$, Equation (19) equals to $\min_\theta W_1(\mathbb{P}_n, \mathbb{P}_\theta; d)$.
- The 1-Lipschitz continuity condition can be relaxed to C-Lipschitz continuity for an arbitrary constant C: In this case, Equation (19) equals to $C \min_\theta W_1(\mathbb{P}_n, \mathbb{P}_\theta; d)$. To enforce this, WGANs clip weights and biases in neural network layers during training.

1-Wasserstein Distance: Wasserstein GAN

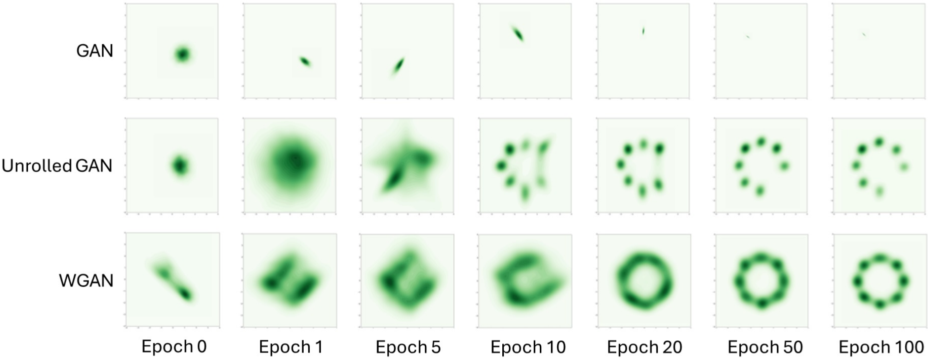

- WGANs performed better than GAN baselines in learning the distribution of Gaussian mixtures with 8 modes.

Images are edited from Arjovsky et al. (2017).

1-Wasserstein Distance: WGAN with Gradient Penalty

2. **WGAN with Gradient Penalty (WGAN-GP)**: Gulrajani et al. (2017) proposed a gradient-based penalty term to enforce the Lipschitz constraint in the dual form.
   - For any $\pi \in \Pi(\mathbb{P}_n, \mathbb{P}_\theta)$ and $0 \le t \le 1$, let $\vec{X}^{(t)} := t\vec{X} + (1-t)\vec{X}'$ where $(\vec{X}, \vec{X}') \sim \pi$. Authors showed that the optimal $1-$Lipschitz continuous function f^* satisfies:

$$\nabla_{\vec{X}^{(t)}} f^*(\vec{X}^{(t)}) = \frac{\vec{X}' - \vec{X}^{(t)}}{\|\vec{X}' - \vec{X}^{(t)}\|} \tag{20}$$

     for any norm $\|\cdot\|$.
   - Motivated by this, authors proposed to target the following:

$$\int f_\phi(\vec{x}) d\mathbb{P}_n(\vec{x}) - \int f_\phi(\vec{x}) d\mathbb{P}_\theta(\vec{x}) + \lambda \left(\int \left(\|\nabla_{\vec{x}} f_\phi(\vec{x})\|_2 - 1 \right)^2 \sum_t (t d\mathbb{P}_n(\vec{x}) + (1-t) d\mathbb{P}_\theta(\vec{x})) \right) \tag{21}$$

p-Wasserstein Distance: Wasserstein Autoencoder

3. **Wasserstein Autoencoder (WAE)**: Tolstikhin et al. (2018) derived an alternative representation of the p-Wasserstein distance (Theorem 1):

$$W_p(\mathbb{P}_n, \mathbb{P}_\theta; d) = \left(\inf_{\mathbb{Q}(\vec{z}|\vec{x}): \int q(\vec{z}|\vec{x}) d\mathbb{P}_n(\vec{x}) = p(\vec{z})} \int d^p(\vec{x}, G_\theta(\vec{z})) d\mathbb{Q}(\vec{z}|\vec{x}) d\mathbb{P}_n(\vec{x}) \right)^{1/p} \tag{22}$$

- Based on this relation, WAEs introduce encoders $q_\phi(\vec{z}|\vec{x})$ and target

$$\theta^* \in \arg\min_\theta \left(\inf_{\phi \in \Phi(\mathbb{P}_n)} \int d^p(\vec{x}, G_\theta(\vec{z})) d\mathbb{Q}_\phi(\vec{z}|\vec{x}) d\mathbb{P}_n(\vec{x}) \right)^{1/p} \tag{23}$$

  where $\Phi(\mathbb{P}_n) := \{\phi \mid \int q_\phi(\vec{z}|\vec{x}) d\mathbb{P}_n(\vec{x}) = p(\vec{z})\}$.
- On the RHS, $q_\phi(\vec{z}|\vec{x})$ can be viewed as an encoder. The constraint in the infimum ensures that the marginal distribution of the posterior distributions matches the prior distributions.

p-Wasserstein Distance: Wasserstein Autoencoder

- In implementation, WAEs introduce a penalty term to enforce the constraint on ϕ. The loss can be expressed as:

$$\int d^p(\vec{x}, G_\theta(\vec{z}))d\mathbb{Q}_\phi(\vec{z}|\vec{x})d\mathbb{P}_n(\vec{x}) + \lambda\mathcal{D}_{\vec{Z}}\left(\int q_\phi(\vec{z}|\vec{x})d\mathbb{P}_n(\vec{x}), p(\vec{z})\right) \tag{24}$$

where $\mathcal{D}_{\vec{Z}}$ indicates the statistical distance applied to the distributions of $\vec{Z}$. WAEs typically use JS divergence and MMD (Maximum Mean Discrepancy) as measures for $\mathcal{D}_{\vec{Z}}$.

p-Wasserstein Distance: Wasserstein Autoencoder

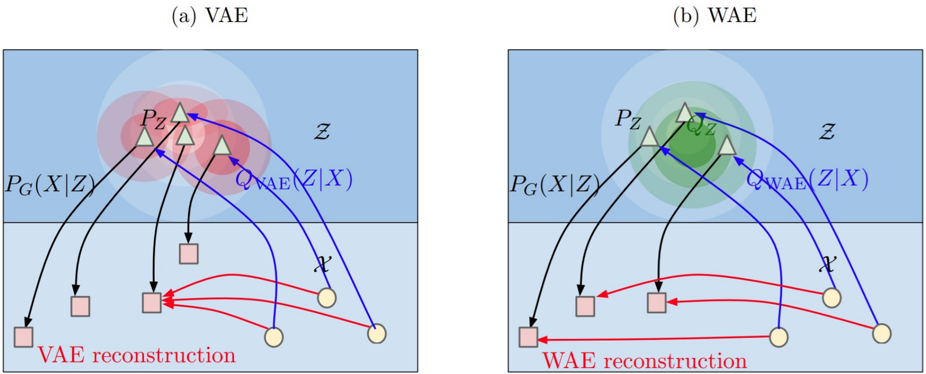

- Compared with the loss of VAEs, the negative ELBO, the penalty term changes from matching $q_\phi(\vec{z}|\vec{x})$ directly with $p(\vec{z})$ to matching $\int q_\phi(\vec{z}|\vec{x})d\mathbb{P}_n(\vec{x})$ with $p(\vec{z})$.

The figure is from Tolstikhin et al. (2018).

Generation Results: WAEs and WGANs

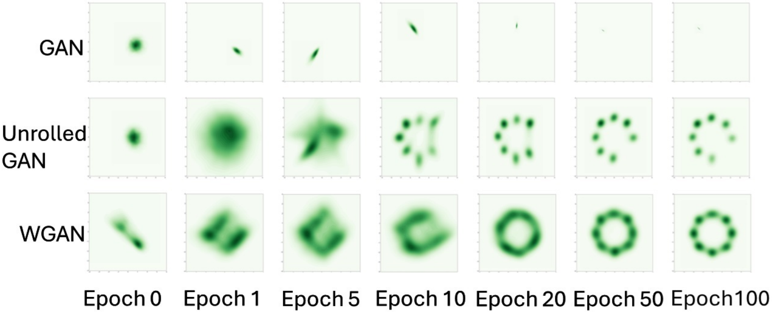

(a) Sharp generation results from WAEs

(b) Preventing mode collapse with WGANs

Images are edited from Arjovsky et al. (2017) and Tolstikhin et al. (2018).

Outline

StarGAN

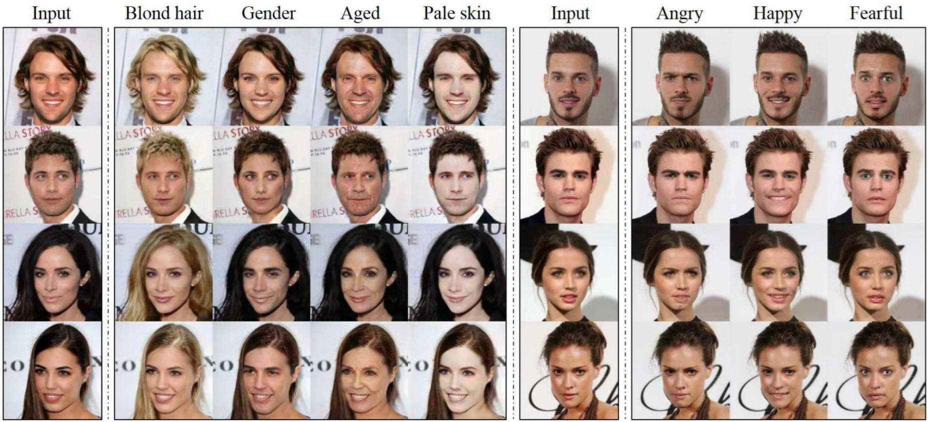

The figure is from Choi et al. (2018).

StarGAN

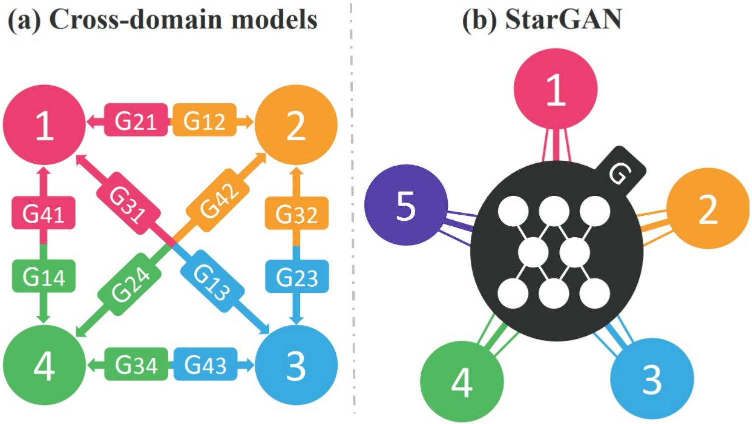

The figure is from Choi et al. (2018).

StarGAN

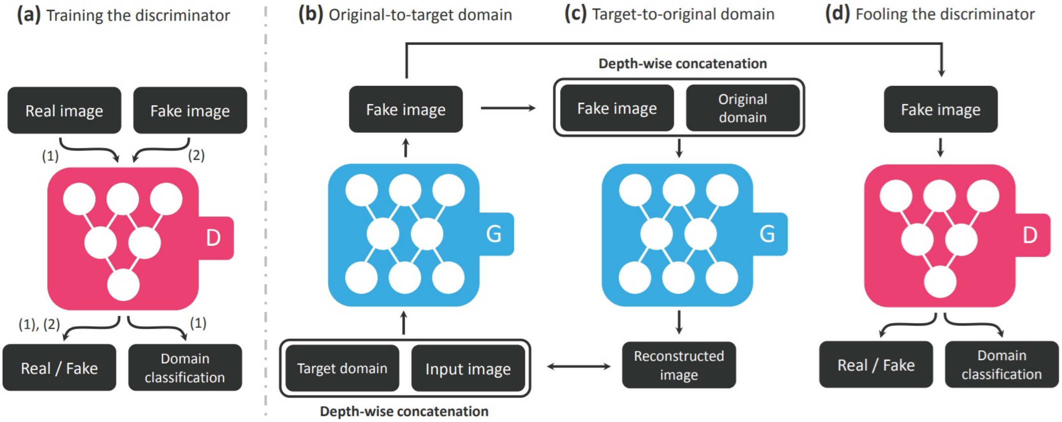

The figure is from Choi et al. (2018).

StarGAN

- Let $G_\theta(\cdot, \vec{c})$ be a translator that moves data from an arbitrary source domain to the target domain described by $\vec{c}$.
- For the adversarial loss component, StarGAN targets:

$$\int f_\phi(\vec{x}) d\mathbb{P}_n(\vec{x}) - \int f_\phi(G_\theta(\vec{x}, \vec{c})) d\mathbb{P}_n(\vec{x}, \vec{c}) \tag{25}$$

  with an added gradient-penalty term.
- With the optimal θ^*, the distribution of $G_{\theta^*}(\vec{X}, \vec{C})$ matches the real distribution, which is a mixture of sub-populations from each data domain.
- The final objective includes classification and cycle-consistency losses to further enforce that, for a given $\vec{c}$, the distribution of $G_{\theta^*}(\vec{X}, \vec{c})$ aligns with the sub-population for corresponding data domain.

StarGAN

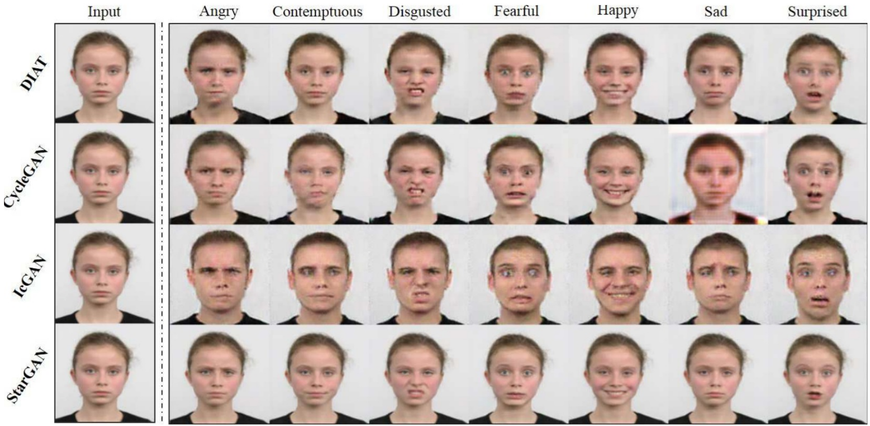

The figure is from Choi et al. (2018).

References I

Arjovsky, M., Chintala, S., and Bottou, L. (2017). Wasserstein generative adversarial networks. In *International conference on machine learning*, pages 214–223. PMLR.

Bickel, P. J. and Freedman, D. A. (1981). Some asymptotic theory for the bootstrap. *The annals of statistics*, 9(6):1196–1217.

Choi, Y., Choi, M., Kim, M., Ha, J.-W., Kim, S., and Choo, J. (2018). Stargan: Unified generative adversarial networks for multi-domain image-to-image translation. In *Proceedings of the IEEE Conference on Computer Vision and Pattern Recognition (CVPR)*.

Freedman, D. A. (1981). Bootstrapping regression models. *The annals of statistics*, 9(6):1218–1228.

Goodfellow, I. (2016). Nips 2016 tutorial: Generative adversarial networks. *arXiv preprint arXiv:1701.00160*.

References II

Gulrajani, I., Ahmed, F., Arjovsky, M., Dumoulin, V., and Courville, A. C. (2017). Improved training of wasserstein gans. *Advances in neural information processing systems*, 30.

Li, C.-L., Chang, W.-C., Cheng, Y., Yang, Y., and Póczos, B. (2017). Mmd gan: Towards deeper understanding of moment matching network. *Advances in neural information processing systems*, 30.

Li, Y., Swersky, K., and Zemel, R. (2015). Generative moment matching networks. In *International conference on machine learning*, pages 1718–1727. PMLR.

Mallows, C. L. (1972). A note on asymptotic joint normality. *The Annals of Mathematical Statistics*, pages 508–515.

Metz, L., Poole, B., Pfau, D., and Sohl-Dickstein, J. (2017). Unrolled generative adversarial networks. In *International Conference on Learning Representations*.

Santambrogio, F. (2015). Optimal transport for applied mathematicians. *Birkäuser, NY*, 55(58-63):94.

References III

Tolstikhin, I., Bousquet, O., Gelly, S., and Schölkopf, B. (2018). Wasserstein auto-encoders. In *Proceedings of the International Conference on Learning Representations (ICLR)*.

Villani, C. (2021). *Topics in optimal transportation*, volume 58. American Mathematical Soc.

Villani, C. et al. (2009). *Optimal transport: old and new*, volume 338. Springer.